

The larger increase in  $\beta_{\text{nuc}}$  with decreasing basicity of the catalyst for  $\text{Me}_2\text{N-R}^+$ , compared with  $\text{MeO-R}^+$  (Figure 11, part C), corresponds to an increase in  $p_{xy} = \partial\beta_{\text{nuc}}/\partial pK_{\text{BH}}$  with decreasing  $\sigma$ . It means that the water-catalyzed reaction of basic alcohols is more significant for the dimethylamino compound and overwhelms the acetate-catalyzed reaction (Figure 5). It follows directly that there is a larger increase in  $\beta_{\text{nuc}}$  with decreasing  $\sigma$  for the water compared with the acetate-catalyzed reaction (Figure 11, part C'). The small value of  $\beta_{\text{nuc}}$  for the acetate-catalyzed reaction with both carbocations makes catalysis detectable with weakly basic alcohols. This represents an increase in  $p_{yy} = \partial\beta_{\text{nuc}}/\partial\sigma$  for the water-catalyzed compared with the acetate-catalyzed reaction. Both of these changes correspond to the third expression of the  $p^*_{xyy}$  coefficient, as shown in eq 16.

$$p^*_{xyy} = \frac{\partial^2\beta_{\text{nuc}}}{\partial\sigma(-\partial pK_{\text{BH}})} = \frac{\partial p_{xy}}{\partial\sigma} = \frac{\partial p_{yy}}{\partial pK_{\text{BH}}} \quad (16)$$

The common terms in eq 14-16 show that these three expressions of the  $p^*_{xyy}$  coefficient are equal to each other. In fact, all of the relationships in eq 14-16 can be obtained directly from eq 17.

$$\frac{\partial^3 \log k}{\partial pK_{\text{BH}}(-\partial pK_{\text{ROH}})(-\partial\sigma)} \quad (17)$$

**Conclusion.** The third-derivative interaction coefficients described here provide a means of characterizing the interrelated changes in transition-state structure and structure-reactivity coefficients that occur as the nature of a reaction mechanism changes. These changes occur as the transition-state structure and structure-reactivity coefficients approach limiting values. They probably also occur for transition states of intermediate structure because the energy surfaces that describe these reactions and their structure-reactivity behavior are not likely to follow simple quadratic equations when changes in transition-state structure are large.

**Registry No.** 4,4'- $\text{H}_3\text{COC}_6\text{H}_4\text{CH}(\text{CH}_3)\text{OCOC}_6\text{H}_4\text{NO}_2$ , 58287-11-9; 4-( $\text{H}_3\text{C}$ ) $_2\text{NC}_6\text{H}_4\text{CH}(\text{CH}_3)\text{OCH}_3$ , 94670-10-7; 4- $\text{H}_3\text{COC}_6\text{H}_4\text{CHCH}_3^+$ , 18207-33-5; 4-( $\text{H}_3\text{C}$ ) $_2\text{NC}_6\text{H}_4\text{CHCH}_3^+$ , 82414-94-6;  $\text{H}_2\text{O}$ , 7732-18-5;  $\text{CF}_3\text{CH}_2\text{OH}$ , 75-89-8;  $\text{Cl}_2\text{CHCH}_2\text{OH}$ , 598-38-9;  $\text{NCCH}_2\text{CH}_2\text{OH}$ , 109-78-4;  $\text{ClCH}_2\text{CH}_2\text{OH}$ , 107-07-3;  $\text{H}_3\text{COCH}_2\text{CH}_2\text{OH}$ , 109-86-4;  $\text{H}_3\text{CC-H}_2\text{OH}$ , 64-17-5;  $\text{HSCH}_2\text{CH}_2\text{CH}_3$ , 107-03-9;  $\text{H}_3\text{CCO}_2^-$ , 71-50-1;  $\text{H}_3\text{CO-CH}_2\text{CO}_2^-$ , 20758-58-1;  $\text{ClCH}_2\text{CO}_2^-$ , 14526-03-5;  $\text{Cl}_2\text{CHCO}_2^-$ , 13425-80-4;  $\text{CF}_3\text{CO}_2^-$ , 14477-72-6.

## General Acid Catalyzed Acetal Hydrolysis. The Hydrolysis of Acetals and Ketals of *cis*- and *trans*-1,2-Cyclohexanediol. Changes in Rate-Determining Step and Mechanism as a Function of pH

Thomas H. Fife\* and R. Natarajan<sup>1</sup>

Contribution from the Department of Biochemistry, University of Southern California, Los Angeles, California 90033. Received January 21, 1986

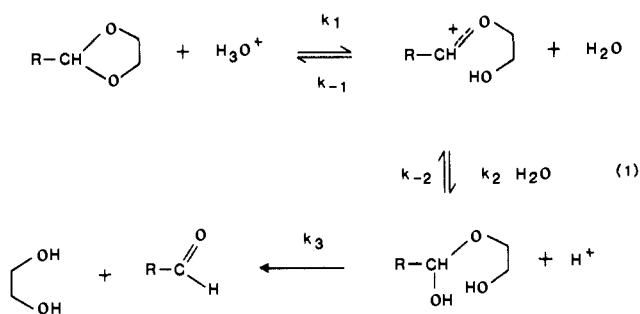
**Abstract:** The plots of  $\log k_{\text{obsd}}$  vs. pH for the hydrolysis of *cis*- and *trans*-1,2-cyclohexanediol isopropylidene ketal in 50% dioxane- $\text{H}_2\text{O}$  (v/v) at 30 °C are linear with slopes of -1.0. The second-order rate constant for hydronium ion catalysis  $k_{\text{H}}$  is five-fold larger with the *trans* derivative than the *cis*, which is very likely due to the increased steric strain in the *trans* configuration. The plot of  $\log k_{\text{obsd}}$  vs. pH for hydrolysis of *cis*-1,2-cyclohexanediol *p*-(dimethylamino)benzylidene acetal in  $\text{H}_2\text{O}$  at 30 °C is pH independent from pH 1 to 4 and linear with a slope of -1.0 at pH >5, quite similar to the profiles of other acetals of *p*-(dimethylamino)benzaldehyde. However, the  $\log k_{\text{obsd}}$ -pH profile for the corresponding *trans* acetal is quite complex and shows seven inflections on the pH scale (1-13) only one of which is due to an ionization (the  $\text{p}K_{\text{a}}$  of the *p*-dimethylamino group conjugate acid). The other six inflections are due to changes in mechanism or rate-determining step as the pH is changed. At pH 1-6 hydronium ion and water-catalyzed hydrolysis of the hemiacetal intermediate is rate determining. At pH >6 attack of  $\text{H}_2\text{O}$  on the oxocarbenium ion intermediate becomes rate limiting, and at pH >7.3  $\text{OH}^-$  attack on the oxocarbenium ion occurs. At pH >8 the rate-determining step changes to hydronium ion catalyzed ring opening ( $k_{\text{H}} = 1.0 \times 10^6 \text{ M}^{-1} \text{ s}^{-1}$  at 30 °C). Ring opening is catalyzed by various general acids with  $\alpha \sim 0.7$ . The plots of  $k_{\text{obsd}}$  vs. buffer concentration are linear with the exception of those determined in carbonate buffer with which there is pronounced curvature due to a change in the rate-determining step with increasing carbonate buffer concentration. The limiting value of  $k_{\text{obsd}}$  at higher buffer concentration is that for attack of  $\text{OH}^-$  on the oxocarbenium ion. At pH >10 the formation of aldehyde is pH independent, which indicates a unimolecular or water-catalyzed decomposition of the acetal. Thus, in the remarkable  $\log k_{\text{obsd}}$  vs. pH profile for hydrolysis of *trans*-1,2-cyclohexanediol *p*-(dimethylamino)benzylidene acetal all of the mechanisms and rate-determining steps for acetal hydrolysis are represented on one plot. This is because of steric strain and the cyclic structure of the acetal, i.e., ring opening is rapid but is nevertheless reversible so that each step becomes rate limiting in turn as pH is increased.

The hydronium ion catalyzed hydrolysis of cyclic acetals proceeds as in eq 1.<sup>2-6</sup> Thus, there are three possible rate-determining steps. Acyclic acetals hydrolyze in the same manner except that

the alcohol leaving group in the initial reaction is expelled into the solvent so that reversibility is minimized. The breakdown of the protonated acetal to a resonance stabilized oxocarbenium ion is generally the rate-determining step in the hydrolysis of simple acetals.<sup>7</sup> General acid catalysis has been observed in the hydrolysis of phenolic acetals with which the leaving group is very good and the oxocarbenium ion is of moderate stability,<sup>8,9</sup> and also in the

(1) Post-doctoral fellow, University of Southern California.  
 (2) Fife, T. H.; Jao, L. K. *J. Org. Chem.* **1965**, *30*, 1492.  
 (3) Ceder, O. *Ark. Kemi* **1954**, *6*, 523.  
 (4) Salomaa, P.; Kankaanpera, A. *Acta Chem. Scand.* **1961**, *15*, 871.  
 Salomaa, P. *Suomen Kemistil. B* **1964**, *B37*, 86.  
 (5) Fife, T. H.; Hagopian, L. *J. Org. Chem.* **1966**, *31*, 1772.  
 (6) Fife, T. H.; Natarajan, R. *J. Am. Chem. Soc.* **1986**, *108*, 2425.

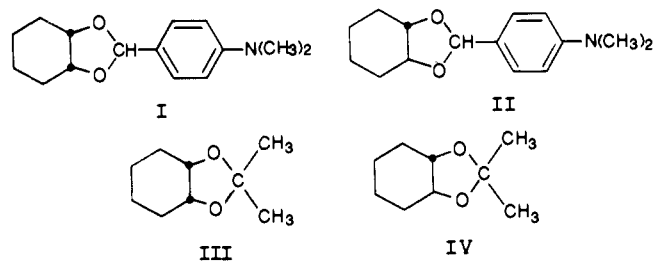
(7) Fife, T. H. *Acc. Chem. Res.* **1972**, *5*, 264.  
 (8) Fife, T. H.; Brod, L. H. *J. Am. Chem. Soc.* **1970**, *92*, 1681. Fife, T. H.; Jao, L. K. *J. Am. Chem. Soc.* **1968**, *90*, 4081.



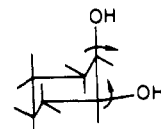
hydrolysis of tropone diethyl ketal<sup>10</sup> with which the intermediate oxocarbenium ion is highly stable. Hemiacetals generally hydrolyze quite rapidly by hydronium ion, hydroxide ion, and water-catalyzed pathways.<sup>11,12</sup> This step is therefore not usually rate determining in the hydrolysis of acetals. However, the hydrolysis of substituted benzaldehyde ethyl hemiacetals is only moderately faster than breakdown of the diethyl acetal at pH < 5.<sup>11,13</sup> Consequently, if the initial breakdown of a substituted benzaldehyde acetal to an oxocarbenium ion could be moderately accelerated in comparison to the corresponding diethyl acetal, then hemiacetal hydrolysis might become rate determining at low pH (< 5).

In the hydrolysis of cyclic acetals the initial C–O bond breaking does not result in departure of the alcohol from the remainder of the molecule; therefore, the possibility of reversibility exists ( $k_{-1}$ ), and attack of a water molecule on the oxocarbenium ion can be rate determining if  $k_{-1} > k_2$  and hemiacetal hydrolysis is fast.<sup>14</sup> It has been recently shown that this is the case in the pH range 5–7.5 in the hydrolysis of 2-(*p*-(dimethylamino)phenyl)-1,3-dioxolane,<sup>6</sup> with which the oxocarbenium ion intermediate is well-stabilized by resonance interaction with the para substituent.<sup>15</sup> At pH > 8 the rate-determining step changes to hydronium ion catalyzed ring opening, and general acid catalysis was detected in the ring opening by very weak buffer acids. This observation was surprising since general acid catalysis was not detectable in the hydrolysis of the analogous acyclic di-*n*-propyl acetal. Thus, a structural feature of the 1,3-dioxolane ring is facilitating general acid catalysis in comparison with analogous acyclic acetals. A detailed study of the general acid-catalyzed reactions of 2-(*p*-(dimethylamino)phenyl)-1,3-dioxolane could not be made because of the pronounced curvature in the plots of  $k_{\text{obsd}}$  vs. buffer concentration.<sup>16</sup> It was thought that a strained cyclic acetal of this parent aldehyde might provide an excellent opportunity for study of the general acid-catalyzed ring opening reaction since the ring-opening would then be more favorable than with the analogous 1,3-dioxolane, and the ease of reversibility would be decreased while maintaining the oxocarbenium ion stabilization. Furthermore, an increased ease of C–O bond breaking in a strained acetal of *p*-(dimethylamino)benzaldehyde might allow hemiacetal breakdown to become rate determining at low pH, in which case all of the possible rate-determining steps in acetal hydrolysis might be directly observed in the reactions of a single acetal. In view of the importance of understanding the factors influencing the rate-determining steps and the general acid-catalyzed reactions in acetal hydrolysis,<sup>17,18</sup> we have therefore investigated the hy-

drolysis of the *cis*- and *trans*-1,2-cyclohexanediol *p*-(dimethylamino)benzylidene acetals I and II. We have also determined rate constants for hydrolysis of the isopropylidene ketals III and IV.



In forming an acetal or ketal derivative of a 1,2-cyclohexanediol the hydroxyl groups must move closer together. In the case of a *cis*-1,2-diol where the groups are axial-equatorial the cyclohexane ring must become more planar, but with a *trans*-1,2-diol



where the groups are equatorial-equatorial the ring must become puckered.<sup>19</sup> We have found in this study that the *trans* derivatives II and IV hydrolyze considerably faster than I and III which have the *cis* configuration, and pronounced general acid catalysis is observed in the hydrolysis of II.

### Experimental Section

**Materials and Methods.** *trans*-1,2-Cyclohexanediol was obtained from Aldrich. *cis*-1,2-Cyclohexanediol was prepared by permanganate oxidation of cyclohexene. Cyclohexene (16.4 g, 0.2 mol) was added to 500 mL of 95% ethanol in a 1 L 3-necked flask. The mixture was cooled at –25 °C by means of a dry ice-acetone bath, and a mixture of MgSO<sub>4</sub> (20.4 g, 0.17 mol) and sodium permanganate monohydrate (27.1 g, 0.17 mol) dissolved in 300 mL of H<sub>2</sub>O was added dropwise over a period of 4 h. The temperature was maintained at –20 to –25 °C during the addition. The mixture was allowed to stand overnight at room temperature. The mixture was then filtered, and the precipitate was washed with ether. The combined filtrate was concentrated by rotary evaporation to a volume of 50 mL and was extracted 3 times with ether. The ether extract was dried over Na<sub>2</sub>SO<sub>4</sub>. The ether was evaporated, and the residue was recrystallized from ethyl acetate. The white crystals melted at 97–98 °C (lit.<sup>20</sup> mp 99 °C).

*p*-(Dimethylamino)benzaldehyde di-*n*-propyl acetal was prepared as previously reported,<sup>6</sup> bp 90–92 °C (0.7 mm). The *cis*- and *trans*-1,2-cyclohexanediol *p*-(dimethylamino)benzylidene acetals I and II were prepared by mixing equivalent amounts of the appropriate diol and *p*-(dimethylamino)benzaldehyde di-*n*-propyl acetal and adding 1 drop of benzoyl chloride (to introduce a trace amount of HCl). The mixture was then heated by means of an oil bath, and the *n*-propyl alcohol formed in the reaction was removed continuously by distillation. The residue was then vacuum distilled. The fraction containing the acetal product was redistilled. *cis*-1,2-Cyclohexanediol *p*-(dimethylamino)benzylidene acetal (I) boiled at 128–130 °C (0.2 mm). The compound solidified upon standing and melted at 45–46 °C and is therefore a pure stereoisomer. Anal. Calcd for C<sub>15</sub>H<sub>21</sub>NO<sub>2</sub>: C, 72.87; H, 8.50. Found: C, 72.46; H, 8.20. *trans*-1,2-Cyclohexanediol *p*-(dimethylamino)benzylidene acetal (II) boiled at 130 °C (0.02 mm). The compound solidified upon standing and melted at 51–52 °C. Anal. Calcd for C<sub>15</sub>H<sub>21</sub>NO<sub>2</sub>: C, 72.87; H, 8.50; N, 5.66. Found: C, 73.06; H, 8.40; N, 5.52.

Acetone diethyl ketal was prepared as previously reported<sup>5</sup> (bp 112–113 °C). The *cis*- and *trans*-1,2-cyclohexanediol isopropylidene ketals III and IV were prepared by mixing equivalent amounts of the appropriate diol and acetone diethyl ketal and adding 1 drop of benzoyl chloride. The mixture was then heated by means of an oil bath, and the ethanol formed in the reaction was removed continuously by distillation. The unreacted acetone diethyl ketal was removed by distillation, and the residue was vacuum distilled. *cis*-1,2-Cyclohexanediol isopropylidene ketal (III) boiled at 51–52 °C (4 mm),  $n_D^{25}$  1.4268 (lit.<sup>21</sup> bp 182 °C (760

(9) Anderson, E.; Capon, B. *J. Chem. Soc. B* **1969**, 1033. Capon, B.; Nimmo, K. *J. Chem. Soc., Perkin Trans 2*, **1975**, 1113.

(10) Anderson, E.; Fife, T. H. *J. Am. Chem. Soc.* **1969**, *91*, 7163.

(11) Przystas, T. J.; Fife, T. H. *J. Am. Chem. Soc.* **1981**, *103*, 4884.

(12) Funderburk, L. H.; Aldwin, L.; Jencks, W. P. *J. Am. Chem. Soc.* **1978**, *100*, 5444.

(13) Jensen, J. L.; Lenz, P. A. *J. Am. Chem. Soc.* **1978**, *100*, 1291. Finley, R. L.; Kubler, D. G.; McClelland, R. A. *J. Org. Chem.* **1980**, *45*, 644.

(14) Willi, A. V. In *Comprehensive Chemical Kinetics*; Bamford, C. H., Tipper, C. F. H., Eds.; Elsevier: Amsterdam, 1977; Vol. 8, pp 49–52.

(15) The  $pK_a$  of the *p*-dimethylamino group conjugate acid is 4–5 so in the pH range 6–7.5 that group is predominantly in the free base form.

(16) These plots indicate that the rate-determining step is changing with increasing buffer concentration.

(17) Fife, T. H. *Adv. Phys. Org. Chem.* **1975**, *11*, 1.

(18) Jencks, W. P. *Chem. Rev.* **1972**, *72*, 705.

(19) Kuhn, L. P. *J. Am. Chem. Soc.* **1952**, *74*, 2492.

(20) Boeseken, J.; van Loon, C. *Proc. Acad. Sci. Amsterdam* **1920**, *23*, 69; *Chem. Abstr.* **1921**, *15*, 237.

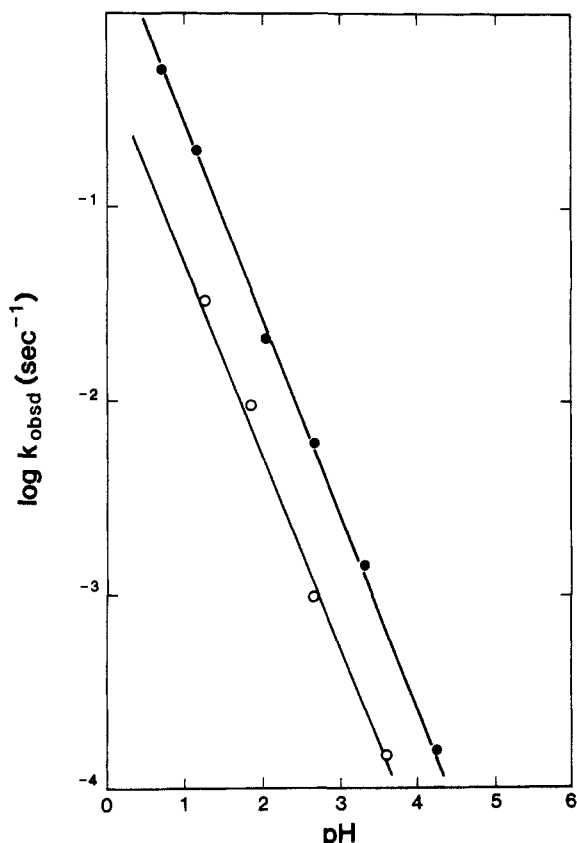


**Figure 1.** Plots of  $\log k_{\text{obsd}}$  vs. pH for hydrolysis of *cis*-1,2-cyclohexanediol isopropylidene ketal (O) and *trans*-1,2-cyclohexanediol isopropylidene ketal (●) in 50% dioxane-H<sub>2</sub>O (v/v) at 30 °C with  $\mu = 0.5$  M with KCl.

mm). *trans*-1,2-Cyclohexanediol isopropylidene ketal (IV) boiled at 65–66 °C (2 mm),  $n_D^{25}$  1.4395 (lit.<sup>22</sup> bp 77–78 °C (20 mm)).

**Kinetic Measurements.** The rates of hydrolysis of compounds I–IV were measured spectrophotometrically with a Beckman Model 25 or a Pye-Unicam SP8-100 spectrophotometer by following the absorbance increase due to appearance of aldehyde or ketone at 360 or 280 nm. The ionic molarity of all buffers was maintained constant at 0.5 M with KCl. Stock solutions of substrate were prepared in anhydrous acetonitrile. Kinetic runs were initiated by injecting 15  $\mu$ L of the substrate stock solution into 3 mL of temperature equilibrated buffer in the cuvette. Reactions that were too rapid to be monitored with a conventional spectrophotometer were followed by using a Durrum Model D-110 stopped-flow spectrophotometer employing methods previously described.<sup>6</sup> The reactions were pseudo first order for at least 4 half-lives. The values of  $k_{\text{obsd}}$ , the pseudo-first-order rate constants, were calculated with an IBM-370 computer. Reaction mixture pH values were measured with a Beckman 3500 digital pH meter.

**Product Isolation.** The isopropylidene ketals III and IV (0.5 g) were completely hydrolyzed in a mixture of 1 mL of H<sub>2</sub>O, 10 mL of methanol, and 2 drops of concentrated HCl. After standing 24 h at room temperature the acid was neutralized with anhydrous Na<sub>2</sub>CO<sub>3</sub>. The mixture was then dried over sodium sulfate and filtered. The methanol was removed by rotary evaporation, and the residue was crystallized from toluene. In each case the respective *cis*- or *trans*-1,2-cyclohexanediol was obtained as shown by the melting point and the lack of depression of the mixture melting point with an authentic sample.

## Results

Plots of  $\log k_{\text{obsd}}$  vs. pH for the hydrolysis of *cis*- and *trans*-1,2-cyclohexanediol isopropylidene ketals (III and IV) in 50% dioxane-H<sub>2</sub>O (v/v) at 30 °C and  $\mu = 0.5$  M are shown in Figure 1. The plots are linear with slopes of  $-1.0$ , which indicates that the reactions are hydronium ion catalyzed. The values of the second-order rate constants  $k_H$  for hydronium ion catalysis are  $0.5 \text{ M}^{-1} \text{ s}^{-1}$  with III and  $2.6 \text{ M}^{-1} \text{ s}^{-1}$  with IV. Buffer catalysis was

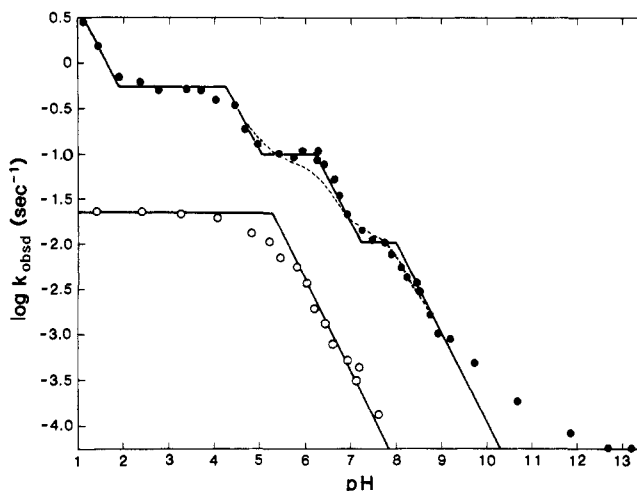


**Figure 2.** Plots of  $\log k_{\text{obsd}}$  vs. pH for hydrolysis of *cis*-1,2-cyclohexanediol *p*-(dimethylamino)benzylidene acetal (O) and *trans*-1,2-cyclohexanediol *p*-(dimethylamino)benzylidene acetal (●) in H<sub>2</sub>O at 30 °C with  $\mu = 0.5$  M with KCl.

**Table I.** Second-Order Rate Constants for Hydronium Ion Catalyzed Hydrolysis of the Cyclic Acetals and Ketals of *cis*- and *trans*-1,2-Cyclohexanediol (I–IV) at 30 °C

compd	$k_H, \text{M}^{-1} \text{s}^{-1}$	$\text{p}K_a$
I	$4.2 \times 10^3$ <sup>a</sup>	5.3
II	$1.0 \times 10^6$ <sup>a,b</sup>	4.3
	$2.4 \times 10^5$ <sup>a,c</sup>	
	$1.0 \times 10^4$ <sup>a,d</sup>	
	$4.2 \times 10^1$ <sup>a,e</sup>	
III	$0.55$ <sup>f</sup>	
IV	$2.6$ <sup>f</sup>	

<sup>a</sup> In H<sub>2</sub>O. <sup>b</sup> At pH > 8 (rate-determining ring opening). <sup>c</sup> At pH 6.2–7.2 (rate-determining attack of H<sub>2</sub>O on the oxocarbenium ion intermediate). <sup>d</sup> At pH 4–5 (rate-determining hemiacetal breakdown (the neutral species)). <sup>e</sup> At pH < 2 (rate-determining hemiacetal breakdown (the conjugate acid)). <sup>f</sup> In 50% dioxane-H<sub>2</sub>O (v/v).

not observed in the hydrolysis of these ketals in formate buffers at concentrations ranging from 0.01 to 0.5 M.

In Figure 2 is shown the plot of  $\log k_{\text{obsd}}$  vs. pH for hydrolysis of *cis*-1,2-cyclohexanediol *p*-(dimethylamino)benzylidene acetal in H<sub>2</sub>O at 30 °C. The plot is pH independent from pH 1 to 4 and linear with a slope of  $-1.0$  at pH > 5 with a  $\text{p}K_{\text{app}}$  of 5.3. The reaction therefore must involve a hydronium ion catalyzed reaction of the neutral species, and  $k_{\text{obsd}}$  is given by eq 2 where  $K_a$  is the

$$k_{\text{obsd}} = k_H a_H \left[ \frac{K_a}{K_a + a_H} \right] \quad (2)$$

apparent dissociation constant and  $k_H$  is the second-order rate constant for hydronium ion catalysis ( $k_H = 4.2 \times 10^3 \text{ M}^{-1} \text{ s}^{-1}$ ). Buffer catalysis was not observed in acetate (pH 4.62) or imidazole buffers (pH 7.05) with the concentrations ranging from 0.01 to 0.5 M.

The plot of  $\log k_{\text{obsd}}$  vs. pH for hydrolysis of *trans*-1,2-cyclohexanediol *p*-(dimethylamino)benzylidene acetal (II) in H<sub>2</sub>O at zero buffer concentration at 30 °C ( $\mu = 0.5$  M) is also shown in Figure 2. The solid lines have been drawn with the limiting slopes of zero and  $-1.0$ . The rate of appearance of aldehyde is much faster than from the *cis* derivative I. The profile is quite complicated in that it reflects both changes in the rate-determining step with changing pH and changes in mechanism (see Discussion). The two regions with slopes of  $-1.0$  at pH < 5 must represent hydronium ion catalyzed hydrolysis of the hemiacetal neutral and protonated species. The pH-independent region from pH 5 to 6.2 (water catalyzed hemiacetal breakdown) is followed by another region of slope  $-1.0$ , which is due to rate-determining attack of water on the oxocarbenium ion intermediate. The attack of OH<sup>-</sup> on the oxocarbenium ion is rate-determining at pH > 7.3, and the

(21) Derx, H. G. *Recl. Trav. Chim.* **1922**, *41*, 312.

(22) Christian, W.; Gogek, C.; Purves, C. *Can. J. Chem.* **1951**, *29*, 911.

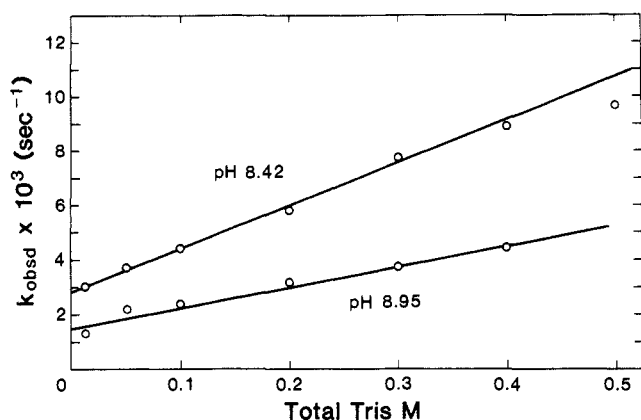


Figure 3. Plots of  $k_{\text{obsd}}$  vs. the total concentration of tris buffer for the hydrolysis of *trans*-1,2-cyclohexanediol *p*-(dimethylamino)benzylidene acetal at pH 8.42 and pH 8.95 ( $\mu = 0.5$  M).

reaction is nearly pH independent. At pH >8 the profile again is linear with a slope of  $-1.0$  because the hydronium ion catalyzed ring opening is rate determining ( $k_{\text{H}} = 1.0 \times 10^6 \text{ M}^{-1} \text{ s}^{-1}$ ). At pH >10 the plot becomes pH independent with  $k_{\text{o}} = 6 \times 10^{-5} \text{ s}^{-1}$ . The experimentally determined rate constants for the hydronium ion catalyzed hydrolysis of I-IV are given in Table I.

The experimental points in Figure 2 for the hydrolysis of II bend downward near pH 6.2 in a much sharper manner than might have been anticipated. The dashed line in the profile shows the trend expected for a change from a pH-independent water reaction to a hydronium ion catalyzed reaction. The experimentally determined value of  $k_{\text{obsd}}$  at pH 6.25 varies from this line by 86%. However, hemiacetal hydrolysis is  $\text{OH}^-$  catalyzed at pH >6,<sup>11</sup> which would influence the observed rate constants in the pH range 5-6. The steady-state equation for  $k_{\text{obsd}}$  in hydrolysis of the neutral species (pH >3), derived from the scheme of eq 1, is given in eq 3 where  $k_3$  is the sum of the rate constants for hemiacetal hy-

$$k_{\text{obsd}} = \left[ \frac{k_1 k_2 k_3 a_{\text{H}}}{k_1 a_{\text{H}} (k_2 + k_{-2} a_{\text{H}} + k_3) + k_{-1} k_{-2} a_{\text{H}} + k_3 (k_{-1} + k_2)} \right] \times \left[ \frac{K_{\text{a}}}{K_{\text{a}} + a_{\text{H}}} \right] \quad (3)$$

drolysis, i.e.,  $k_3 = (k_{\text{H}}' a_{\text{H}} + k_{\text{o}}' + k_{\text{OH}}'(\text{OH}^-))$ ,  $k_{\text{H}}'$  is the second-order rate constant for hydronium ion catalyzed hemiacetal hydrolysis,  $k_{\text{o}}'$  is the rate constant for water catalyzed hemiacetal hydrolysis, and  $k_{\text{OH}}'$  is the second-order rate constant for  $\text{OH}^-$  catalyzed hemiacetal breakdown. Employing this equation and appropriate values of the constants,  $k_{\text{H}}' = 1.0 \times 10^4 \text{ M}^{-1} \text{ s}^{-1}$ ,  $k_{\text{OH}}' = 8 \times 10^6 \text{ M}^{-1} \text{ s}^{-1}$ ,  $k_1 = 1.0 \times 10^6 \text{ M}^{-1} \text{ s}^{-1}$ ,  $k_{-1} = 7.5 \times 10^3 \text{ s}^{-1}$ ,  $k_2 = 2.4 \times 10^3 \text{ s}^{-1}$ ,  $k_{\text{o}}' = 0.08 \text{ s}^{-1}$ , and  $k_{-2} = 4 \times 10^4 \text{ M}^{-1} \text{ s}^{-1}$ , a good fit of the experimental points to the solid theoretical line in Figure 2 can be obtained in the pH range 3-7 including the downward bend at pH 6.2. The values of  $k_{\text{H}}'$ ,  $k_{\text{o}}'$ , and  $k_{\text{OH}}'$  are in reasonable accord with the constants obtained by extrapolation of the Hammett  $\sigma$  plots for the hydrolysis of substituted benzaldehyde ethyl hemiacetals to  $\sigma = -0.8$ .<sup>11</sup> The other constants were calculated as outlined in the Discussion. As the pH is increased  $k_{\text{OH}}'(\text{OH}^-)$  will become large so that the hemiacetal breakdown will be rapid. Near pH 6  $k_{\text{o}}' + k_{\text{OH}}'(\text{OH}^-)$  is greater than  $k_{-2} a_{\text{H}}$ , and  $k_3 (k_{-1} + k_2)$  becomes greater than  $k_1 k_2 a_{\text{H}}$  so that attack of  $\text{H}_2\text{O}$  on the oxocarbenium ion ( $k_2$ ) becomes the rate-determining step. A sharp break in the profile will then occur at pH 6.2.

At pH 7.3 the mechanism changes to rate-determining attack of  $\text{OH}^-$  on the oxocarbenium ion intermediate. As the pH increases a further change in rate-determining step to ring opening must then occur. The fit of the experimental  $k_{\text{obsd}}$  values to eq 3 is extended to pH 9 upon substituting  $k_2'$  for  $k_2$ , where  $k_2'$  is the sum of the rate constants for reaction of the oxocarbenium ion intermediate with  $\text{H}_2\text{O}$  and  $\text{OH}^-$ , i.e.,  $k_2' = (k_2 + k_{\text{OH}}(\text{OH}^-))$

Table II. Second-Order Rate Constants for General Acid Catalysis in the Hydrolysis of *trans*-1,2-Cyclohexanediol *p*-(Dimethylamino)benzylidene Acetal in  $\text{H}_2\text{O}$  at 30 °C with  $\mu = 0.5$  M

conjugate acid	pK <sub>a</sub>	k <sub>HA</sub> , M <sup>-1</sup> s <sup>-1</sup>
2,6-Lutidine	6.6	0.20
phosphate	6.8	0.26
<i>N</i> -ethylmorpholine	7.8	0.03
tris	8.2	0.04
morpholine	8.6	0.25
<i>N</i> -methylpiperidine	10.0	0.001
carbonate	10.2	0.044

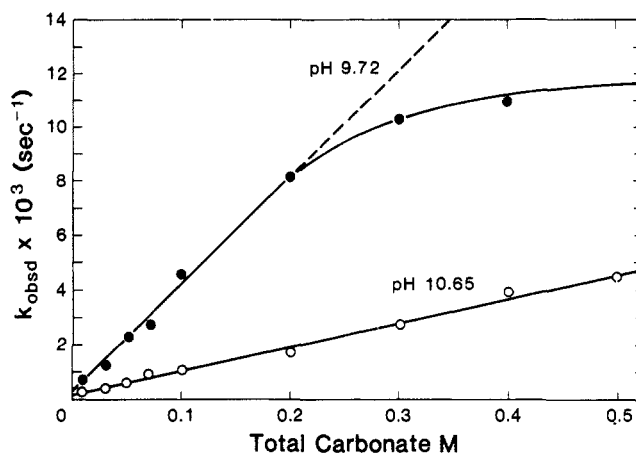


Figure 4. Plots of  $k_{\text{obsd}}$  vs. the total concentration of carbonate buffer for the hydrolysis of *trans*-1,2-cyclohexanediol *p*-(dimethylamino)benzylidene acetal at pH 9.72 and pH 10.65 ( $\mu = 0.5$  M).

and  $k_{\text{OH}} = 6 \times 10^9 \text{ M}^{-1} \text{ s}^{-1}$ . The dashed line in Figure 2 in the pH region near 8 was calculated by employing eq 4, which follows

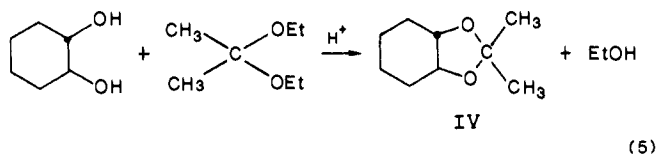
$$k_{\text{obsd}} = \frac{k_1 k_2 a_{\text{H}} + k_1 k_{\text{OH}} K_{\text{W}}}{k_{-1} + k_2 + k_{\text{OH}}(\text{OH}^-)} \quad (4)$$

from eq 3 at pH >7, where  $K_{\text{W}}$  is the ion product of water ( $K_{\text{W}} = 1.47 \times 10^{-14}$  at 30 °C). Equation 4 encompasses the change in mechanism at pH >7 and illustrates why the rate-determining step must change as the  $\text{OH}^-$  concentration becomes large. In the pH region above 9  $k_{\text{obsd}} = (k_1 a_{\text{H}} + k_{\text{o}})$  where  $k_{\text{o}}$  is the rate constant for pH-independent ring opening.

Pronounced buffer catalysis was observed in the hydrolysis of II at pH >6. In Figure 3 plots are shown of  $k_{\text{obsd}}$  vs. the total concentration of tris buffer at two constant pH values. The slope increases as the pH is decreased showing that the acid component of the buffer is catalytically active. Linear plots were also obtained in 2,6-lutidine, phosphate, *N*-ethylmorpholine, morpholine, *n*-butylamine, and *N*-methylpiperidine buffers. The second-order rate constants  $k_{\text{HA}}$  for general acid catalysis are given in Table II. The plots of  $k_{\text{obsd}}$  vs. buffer concentration were markedly curved with carbonate buffers. The plots of  $k_{\text{obsd}}$  vs. carbonate concentration at two constant pH values are shown in Figure 4.

## Discussion

It was at one time thought that an isopropylidene ketal could only be formed from a 1,2-cyclohexanediol when the hydroxyl groups had the *cis* configuration.<sup>20,23</sup> However, it was later found that such ketals could also be prepared from *trans*-1,2-cyclohexanediol if forcing conditions were employed.<sup>22</sup> In view of the relative difficulty of preparation of the *trans* derivative it is probable that steric strain exists in such ketals.<sup>19</sup> In the present work *trans*-1,2-cyclohexanediol isopropylidene ketal (IV) was synthesized by an acetal interchange reaction with acetone diethyl ketal in which the reaction was driven to completion by the distillation of ethanol from the reaction mixture (eq 5). Likewise, *trans*-1,2-cyclohexanediol *p*-(dimethylamino)benzylidene acetal



(II) was prepared from *p*-(dimethylamino)benzaldehyde dipropyl acetal in a similar manner.

The second-order rate constant  $k_H$  for hydronium ion catalyzed hydrolysis of *cis*-1,2-cyclohexanediol isopropylidene ketal (III) is  $0.55 \text{ M}^{-1} \text{ s}^{-1}$  at  $30^\circ \text{C}$  in 50% dioxane– $\text{H}_2\text{O}$  (v/v), which is larger than the  $k_H$  for hydrolysis of 2,2-dimethyl-1,3-dioxolane under the same conditions ( $0.076 \text{ M}^{-1} \text{ s}^{-1}$ ).<sup>5,24</sup> Thus, there is some apparent instability associated with the cyclic ketal when the five-membered ring of III is fused *cis* (a,e) to the cyclohexane ring. The *trans* fused compound (e,e), however, has a  $k_H$  value that is five-fold larger than that of III, which is indicative of a greater degree of ring strain.

*cis*-1,2-Cyclohexanediol *p*-(dimethylamino)benzylidene acetal (I) hydrolyzes with a second-order rate constant  $k_H$  that is comparable to that for hydrolysis of 2-(*p*-(dimethylamino)phenyl)-1,3-dioxolane.<sup>6</sup> The hydrolysis of the latter acetal proceeds with rate-determining attack of  $\text{H}_2\text{O}$  on the oxocarbenium ion produced by ring opening at  $\text{pH} < 7.5$ , although the rate constants for that reaction are only slightly less (threefold) than those for hydronium ion catalyzed ring opening. The shape of the  $\log k_{\text{obsd}}$  vs. pH profile for the hydrolysis of I is similar to that for hydrolysis of the corresponding dipropyl acetal and the 1,3-dioxolane at  $\text{pH} < 7.5$ , but the apparent  $\text{pK}_a$  of I (5.3) is higher than that of the 1,3-dioxolane (4.7). The  $\text{pK}_{\text{app}}$  may therefore be influenced by a change in the rate-determining step near  $\text{pH} 5$ . As is the case with III, there is no indication of any large strain effects in the hydrolysis reaction of I. However, the corresponding *trans* derivative II hydrolyzes quite fast relative to I, again indicating strain in the *trans* configuration. The difference in  $k_H$  values for I and II is much larger than with III and IV, which is very likely due to different mechanisms in the ring opening process. The hydrolysis of II (ring opening) is general acid catalyzed, i.e., C–O bond breaking and proton transfer very likely occur in a concerted process.<sup>7</sup> In contrast, the reactions of I, III, and IV are not general acid catalyzed, and the mechanism of ring opening probably involves preequilibrium protonation followed by rate-determining C–O bond breaking. Thus, there should be more C–O bond breaking in the transition state for II relative to I than for IV relative to III, and consequently the rate enhancement due to relief of steric strain should be larger in the ring opening of II than IV.

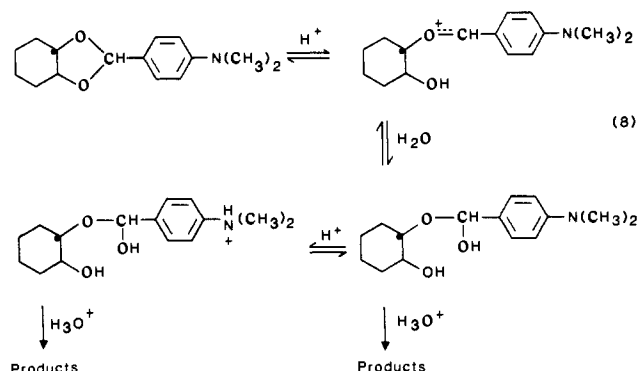
The plot of  $\log k_{\text{obsd}}$  (extrapolated to zero buffer concentration) vs. pH for hydrolysis of *trans*-1,2-cyclohexanediol *p*-(dimethylamino)benzylidene acetal (II) in Figure 2, is quite complicated. There are seven inflections in this profile, only one of which can be due to an ionization. The values of  $k_{\text{obsd}}$  are quite large in comparison with the *cis* derivative (I) or even the corresponding dipropyl acetal, which has  $k_H = 7 \times 10^4 \text{ M}^{-1} \text{ s}^{-1}$  at  $30^\circ \text{C}$ .<sup>6</sup> Thus, it is clear that the ring-opening reaction of II is rapid and that other steps in the reaction sequence have become rate limiting. Since ring opening of a cyclic acetal may be reversible (eq 1), either attack of a water molecule on the oxocarbenium ion intermediate ( $k_2$ ) or hemiacetal breakdown ( $k_3$ ) can be rate determining if the ring reclosure is competitive with the reaction of the intermediate with water. The equation for  $k_{\text{obsd}}$  will then be eq 6, considering hemiacetal hydrolysis to be fast. If  $k_{-1} \gg k_3$ , then eq 7 is obtained, and attack of  $\text{H}_2\text{O}$  on the oxocarbenium

$$k_{\text{obsd}} = \left( \frac{k_1 k_2 (\text{H}_2\text{O})}{k_{-1} (\text{H}_2\text{O}) + k_2 (\text{H}_2\text{O})} \right) a_{\text{H}} \quad (6)$$

$$k_{\text{obsd}} = \left( \frac{k_1 k_2}{k_{-1}} \right) a_{\text{H}} \quad (7)$$

ion will be rate limiting if hemiacetal breakdown is rapid. On the other hand, hemiacetal breakdown can be rate determining if  $k_{-2} a_{\text{H}} > k_3$ . Hemiacetal hydrolysis at  $\text{pH} > 5$  is water catalyzed and then  $\text{OH}^-$  catalyzed.<sup>11</sup> As a consequence, hemiacetal hydrolysis can only be rate determining at  $\text{pH}$  less than 6, since only at low  $\text{pH}$  can the condition  $k_{-2} a_{\text{H}} > k_3$  ( $\text{H}_2\text{O}$  or  $\text{OH}^-$ ) be fulfilled. Hemiacetal hydrolysis can also be rate determining at low  $\text{pH}$  if the ring opening is very rapid and the reactions are not exceptionally reversible, i.e.,  $k_1 k_2 a_{\text{H}}$  is large ( $k_1 k_2 > k_{-1} k_{-2}$ ). This possibility would be most likely at low  $\text{pH}$  in reactions of a strained acetal.<sup>25</sup> In the hydrolysis of substituted benzaldehyde diethyl acetals decomposition of the protonated acetal to an oxocarbenium ion is rate determining at all  $\text{pH}$  values, but the rate of hemiacetal hydrolysis is only moderately faster than oxocarbenium ion formation at  $\text{pH} < 5$ .<sup>11,13</sup> In the case of II the fast rate of ring opening has led to a situation in which hemiacetal hydrolysis is very likely rate determining at  $\text{pH} < 5$ .

The two hydronium ion catalyzed reactions of II at low  $\text{pH}$  ( $< 5$ ) are not observed in the hydrolysis of I nor in the hydrolysis of the corresponding 1,3-dioxolane or the dipropyl acetal.<sup>6</sup> The  $\text{pH}$ -independent reaction at  $\text{pH} < 5$  in the hydrolysis of those acetals is due to a hydronium ion catalyzed reaction of the neutral species at  $\text{pH}$  values where the protonated species (protonated dimethylamino group) is predominant. From the Hammett  $\rho$  value of  $-3.35$  for hydrolysis of diethyl acetals and 1,3-dioxolane derivatives of substituted benzaldehydes and the  $\sigma$  values for neutral and protonated dimethylamino groups, a  $10^5$  difference would be expected in the second-order rate constants for hydronium ion catalyzed ring opening of the neutral and protonated species.<sup>6</sup> The  $\rho$  value for hydronium ion catalyzed hemiacetal breakdown is, however,  $-1.9$ .<sup>11</sup> As a consequence, there should only be  $10^3$  difference in the second-order rate constants for the species, and both reactions should be detected on the  $\text{pH}$  scale. Therefore, it is highly likely that the reactions of II at low  $\text{pH}$  involve hydronium ion catalyzed breakdown of the neutral and protonated species of the hemiacetal intermediate (eq 8). The apparent  $\text{pK}_a$

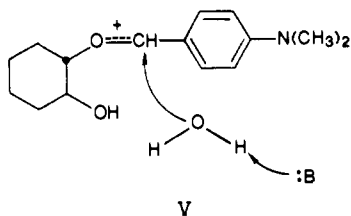


of 4.3 is close to that which would be expected for the *p*-dimethylamino group conjugate acid.<sup>6</sup> At  $\text{pH} > 5$  the reaction becomes  $\text{pH}$  independent, which very likely reflects water catalyzed hemiacetal hydrolysis.

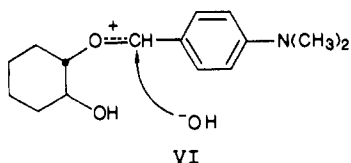
The downward bend in the profile of Figure 2 at  $\text{pH} 6.2$  must represent a change in the rate-determining step since there is no substituent group in the molecule that could reasonably be expected to have a  $\text{pK}_a$  in that  $\text{pH}$  region, i.e., the downward bend in the profile cannot be attributed to an ionization. The sharpness of the downward bend of the experimental points near  $\text{pH} 6.2$  is very likely due to the fact that hemiacetal hydrolysis begins to be  $\text{OH}^-$  catalyzed in that  $\text{pH}$  range.<sup>11</sup> Consequently, the observed rate constants do not decline with increasing  $\text{pH}$  until the rate-determining step has completely changed and  $k_{\text{obsd}}$  is no longer greatly influenced by hemiacetal breakdown. The lack of a pronounced transition region near  $\text{pH} 6$  is predicted by eq 3. Thus, the sharp break in the profile at  $\text{pH} 6.2$  provides support for rate-determining hemiacetal hydrolysis below  $\text{pH} 6$ . The new rate-determining step must be attack of water on the oxocarbenium ion intermediate ( $k_2$ ). The only alternative interpretation would be that ring opening has become rate limiting at  $\text{pH} 6.2$ , but it

(24) Acetone diethyl ketal hydrolyzes considerably faster under these conditions  $k_H = 1370 \text{ M}^{-1} \text{ s}^{-1}$  at  $30^\circ \text{C}$ .<sup>5</sup>

would then not be possible to reasonably explain the further changes in the plot of  $\log k_{\text{obsd}}$  vs. pH as pH is increased. A second change in the rate-determining step occurs at  $\text{pH} > 8$ , and it is that step that must reflect the hydronium ion catalyzed ring opening. The changes in the profile at  $\text{pH} > 7.3$  indicate strongly that attack of water on the oxocarbenium ion must be rate limiting in the pH range 6–7.3. The second-order rate constants for catalysis by 2,6-lutidine and  $\text{H}_2\text{PO}_4^-$  in Table II were obtained at pH values less than 7. The catalysis in those buffers then is very likely general base catalysis of the attack of water following the acid-catalyzed ring-opening step (V).



At pH 7.3 the reaction again becomes nearly pH independent as the mechanism changes to rate-determining attack of  $\text{OH}^-$  on the oxocarbenium ion intermediate. Rate-determining attack of  $\text{OH}^-$  on the oxocarbenium ion intermediate (VI) following the



hydronium ion catalyzed ring opening would be pH independent. The  $\text{OH}^-$  catalyzed reaction (VI) is also rate determining at high buffer concentrations (carbonate buffer at pH 9.72). The value of  $k_{\text{obsd}}$  for this reaction will then be given by eq 9. If the reaction

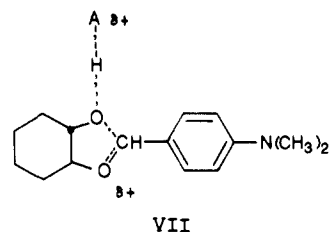
$$k_{\text{obsd}} = \frac{k_1 k_{\text{OH}} K_w}{k_{-1}} \quad (9)$$

is considered to be diffusion controlled ( $k_{\text{OH}} = 6 \times 10^9 \text{ M}^{-1} \text{ s}^{-1}$ ),<sup>26,27</sup> then since  $k_1 = 1.0 \times 10^6 \text{ M}^{-1} \text{ s}^{-1}$ ,  $k_{-1}$  must equal  $7.5 \times 10^3 \text{ s}^{-1}$ . One may then calculate  $k_2$  since in the pH range 6.2–7 eq 10 holds;

$$k_{\text{obsd}} = \frac{k_1 k_2 a_{\text{H}}}{k_{-1} + k_2} \quad (10)$$

$k_2$  then equals  $2.4 \times 10^3 \text{ s}^{-1}$ , and the ratio  $k_{-1}/k_2$  is 3, i.e., the reversibility of ring opening is an important feature of these reactions even though the acetal is strained and the ring opens rapidly. Note that even if the absolute values of the constants differ somewhat because of the value chosen for  $k_{\text{OH}}$ , the ratio of  $k_{-1}/k_2$  will remain the same. The pH-independent value of  $k_{\text{obsd}}$  for the  $\text{OH}^-$ -catalyzed reaction VI in the hydrolysis of II ( $k_{\text{obsd}}'' \sim 0.01 \text{ s}^{-1}$ ) is 50-fold larger than the comparable rate constant for hydrolysis of 2-(*p*-(dimethylamino)phenyl)-1,3-dioxolane.<sup>6</sup> Since the oxocarbenium ions derived from the two compounds are of similar stability, the much larger rate constant of II must reflect the different ratios of  $k_{-1}/k_1$ . As the pH is increased the rate of the reaction VI will increase so that at some pH it will be faster than the rate of the ring reclosure. The rate-determining step must then change to ring opening when  $k_{\text{OH}}(\text{OH}^-)$  is greater than  $k_{-1}$ . This occurs near pH 8.2.

**General Acid Catalysis in Ring Opening.** At pH 8.2 the plot of  $\log k_{\text{obsd}}$  vs. pH again becomes linear with a slope of  $-1.0$ . This reaction corresponds to hydronium ion catalyzed ring opening. The ring opening reaction is catalyzed by general acids (Figures 3 and 4) and most likely involves partial proton transfer to the leaving group (VII) analogous to the general acid-catalyzed hy-



drolisis reactions of acetals and ketals that have been previously observed.<sup>7–10</sup> General acid catalysis is only found in acetal hydrolysis when C–O bond breaking is facile due to a good leaving group or to an oxocarbenium ion that is highly stabilized.<sup>7</sup> The *p*-(dimethylamino)phenyl group provides reasonably good stabilization of the intermediate by a resonance interaction. This degree of oxocarbenium ion stabilization is clearly necessary,<sup>29</sup> as indicated by the lack of general acid catalysis in the hydrolysis of the isopropylidene ketals III and IV. However, the oxocarbenium ion stabilization effects are not sufficient by themselves to give rise to general acid catalysis; such catalysis is not detected in the hydrolysis of the analogous di-*n*-propyl acetal,<sup>6</sup> nor in the hydrolysis of the *cis*-1,2-cyclohexanediol acetal I. The pronounced general acid catalysis in the ring opening of the *trans*-1,2-cyclohexanediol acetal II, in contrast with the lack of such catalysis in the hydrolysis of I, must be due to the increased ease of C–O bond breaking brought about by steric strain in the reactant, which will allow proton transfer to the leaving group to become part of the rate-determining step, as in VII.<sup>7,25</sup>

The plots of  $k_{\text{obsd}}$  vs. buffer concentration in the ring opening of 2-(*p*-(dimethylamino)phenyl)-1,3-dioxolane are markedly curved.<sup>6</sup> The buffer independent reactions at high buffer concentrations all have nearly the same values of  $k_{\text{obsd}}$  and reflect a change in rate-limiting step to rate-determining attack of  $\text{OH}^-$  on the oxocarbenium ion. The rate-determining step changes at high buffer concentration because of general base catalysis in the ring-closure step,  $k_{-1} + k_{-1}'(\text{B}) > k_{\text{OH}}(\text{OH}^-)$ . In contrast, the plots of  $k_{\text{obsd}}$  vs. buffer concentration in the hydrolysis of II are nicely linear, as in Figure 3 (with the exception of those determined in carbonate buffer), because at the highest buffer concentration studied (0.5 M),  $k_{-1}'(\text{B})$  has still not attained the value required to change the rate-determining step. From the second-order rate constants for general acid catalysis in Table II, obtained from the linear plots of  $k_{\text{obsd}}$  vs. buffer acid concentration, there would appear to be little systematic correlation between the rate constants and the  $\text{p}K_{\text{a}}$  of the general acid. However, the analysis of the Brønsted relationship is made difficult by the fact that general acid catalysis in ring opening could only be studied over a span of 2–3 pH units (8–10.5). Rate constants were determined for five general acids, but these differ considerably in type. Employing the second-order rate constants for the conjugate acids of *N*-ethylmorpholine and *N*-methylpiperidine, which are both tertiary amines, a Brønsted  $\alpha$  coefficient of 0.7 was calculated.<sup>30</sup> The  $\alpha$  value indicates a reaction involving concerted C–O bond breaking and proton transfer from the general acid (mechanism VII) with proton transfer reasonably well advanced in the transition state. It might be noted that  $\text{HCO}_3^-$  is a better general acid than would have been anticipated on the basis of its  $\text{p}K_{\text{a}}$ . The marked curvature of the plots of  $k_{\text{obsd}}$  vs. carbonate buffer concentration is due to a change in rate-determining step, and it will be noted that the value of  $k_{\text{obsd}}$  at high buffer concentration is the same as that for the pH-independent region of the  $\log k_{\text{obsd}}$

(25) Atkinson, R. F.; Bruce, T. C. *J. Am. Chem. Soc.* **1974**, *96*, 819 and references therein.

(26) The reaction of sulfite anion with substituted phenylethyl-1-methoxy cations proceeds at a near diffusion-controlled rate. Young, P. R.; Jencks, W. P. *J. Am. Chem. Soc.* **1977**, *99*, 8238.

(27) The rate constant for reaction of water with the comparably stable (*p*-(dimethylamino)phenylethyl)-1-methoxy cation has been estimated at  $5 \times 10^3 \text{ M}^{-1} \text{ s}^{-1}$  at 25 °C. Richard, J. P.; Rothenberg, M. E.; Jencks, W. P. *J. Am. Chem. Soc.* **1984**, *106*, 1361. Employing the  $N^+$  value<sup>28</sup> for  $\text{OH}^-$  (4.5), the  $k_{\text{OH}}$  value for attack of  $\text{OH}^-$  on that cation would then be  $8 \times 10^9 \text{ M}^{-1} \text{ s}^{-1}$ .

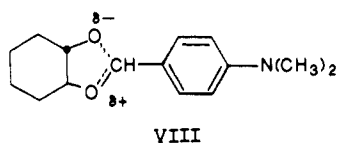
(28) Ritchie, C. D.; Virtanen, P. O. I. *J. Am. Chem. Soc.* **1972**, *94*, 4966.

(29) Fife, T. H.; Anderson, E. *J. Org. Chem.* **1971**, *36*, 2357.

(30) Brønsted  $\alpha$  coefficients between 0.5 and 0.7 have been obtained in acetal hydrolysis reactions where a substituted phenol is the leaving group.<sup>8,9</sup>

vs. pH profile (zero buffer) in Figure 2 in the pH region from 7.5 to 8.0, i.e., that for rate-limiting attack of OH<sup>-</sup> on the oxocarbenium ion.

At pH > 10 the ring opening reaction becomes independent of pH. Similar pH-independent reactions have been found in the hydrolysis of acetals and ketals subject to general acid catalysis.<sup>7,8,10</sup> These reactions involve rate-determining unimolecular C–O bond breaking.<sup>8</sup> Thus the analogous reaction of II may also involve a unimolecular decomposition (VIII). Such a reaction would be



due to the significant oxocarbenium ion stabilization and the ease of C–O bond breaking brought about by relief of steric strain in the acetal of *trans*-1,2-cyclohexanediol. An alternative possibility is that water is acting as a general acid, which would require a second-order rate constant of  $1.1 \times 10^{-6} \text{ M}^{-1} \text{ s}^{-1}$  ( $k_0/55.5 \text{ M}$ ). This second-order rate constant fits reasonably well on a Brønsted plot of slope  $-0.7$  including points for the general acids and hydronium ion.

In summary, in the plot of  $\log k_{\text{obsd}}$  vs. pH for the hydrolysis of *trans*-1,2-cyclohexanediol *p*-(dimethylamino)benzylidene acetal in H<sub>2</sub>O there are seven inflections, only one of which is due to an ionizable group (the *p*-dimethylamino group conjugate acid). As discussed, the other inflections are produced by two changes

in rate-determining step and four changes in mechanism as pH is increased. This novel situation comes about because of steric strain in the acetal, so that ring opening is rapid, and the cyclic structure of the acetal, which can lead to reversibility of ring opening. The resultant compromise between these opposing factors is one in which each step becomes rate limiting in turn as pH is increased. Hemiacetal breakdown can only be rate determining at pH < 6 because of OH<sup>-</sup> catalysis at higher pH. Rate-limiting hydrolysis of the protonated and neutral species of the hemiacetal at low pH is brought about because of the rapid hydronium ion catalyzed ring opening or  $k_{-2}a_{\text{H}} > k_3$ . As the pH is increased above 6 attack of a water molecule on the oxocarbenium ion intermediate becomes rate limiting because at those pH values the hydroxide ion catalyzed breakdown of the hemiacetal is rapid with  $k_3(\text{OH}^-) > k_{-2}a_{\text{H}}$ . The mechanism changes at pH > 7 to attack of OH<sup>-</sup> on the oxocarbenium ion, and as the concentration of OH<sup>-</sup> becomes larger the hydronium ion catalyzed ring opening becomes rate determining, i.e.,  $k_{\text{OH}}(\text{OH}^-) > k_{-1}$ . The ring-opening is also catalyzed by general acids. Finally at pH > 10 the mechanism changes to pH-independent rate-determining ring opening. Thus, all of the mechanisms and rate-determining steps for the hydrolysis of an acetal are represented on one remarkable  $\log k_{\text{obsd}}$  vs. pH profile (Figure 2).

**Acknowledgment.** This work was supported by a research grant from the National Institutes of Health.

**Registry No.** I, 103457-39-2; II, 103457-40-5; III, 41564-26-5; IV, 24148-95-6.

## Structure Elucidation of the Antibiotic Desertomycin through the Use of New Two-Dimensional NMR Techniques

Ad Bax,<sup>\*†</sup> A. Aszalos,<sup>‡</sup> Z. Dinya,<sup>§</sup> and K. Sudo<sup>†±</sup>

*Contribution from the Laboratory of Chemical Physics, National Institute of Arthritis, Diabetes, and Digestive and Kidney Diseases, National Institutes of Health, Bethesda, Maryland 20892, the Division of Drug Biology, Food and Drug Administration, Washington, D.C. 20204, and the Antibiotics Research Laboratory, Kossuth University, Debrecen, Hungary.*

Received March 20, 1986

**Abstract:** The structure of the antibiotic desertomycin has been determined by using modern two-dimensional NMR techniques. Mass spectroscopy indicated a *M*, of 1192. All other structural information was obtained from <sup>1</sup>H and <sup>13</sup>C NMR. <sup>1</sup>H–<sup>1</sup>H double-quantum-filtered COSY and homonuclear Hartmann–Hahn spectroscopy in combination with heteronuclear shift correlation and <sup>1</sup>H-detected heteronuclear multiple-bond multiple-quantum coherence were used for obtaining all crucial connectivities required for establishing the structure. Complete <sup>1</sup>H and <sup>13</sup>C assignments are also presented. The apparent molecular formula of desertomycin was determined as C<sub>61</sub>H<sub>109</sub>NO<sub>21</sub>.

Isolation of desertomycin, a broad-spectrum antibiotic, was reported first by Uri et al.<sup>1</sup> in 1958. Preliminary structural work indicated the presence of a mannose moiety in the antibiotic.<sup>2</sup> Some physicochemical characteristics and a (erroneous) molecular formula of C<sub>57</sub>H<sub>109</sub>NO<sub>24</sub> were reported by Dolak et al.<sup>3</sup> in 1983. Interesting biological properties of desertomycin such as blockage of K<sup>+</sup> channels in muscle fibers,<sup>4</sup> selective isolation of human pathogenic fungi in culture,<sup>5</sup> and cytotoxicity against leukemia cells<sup>6</sup> also have been reported. Because of these interesting properties, we have undertaken the structure elucidation of desertomycin. Repeated initial attempts to grow crystals suitable

for X-ray diffraction studies failed, forcing us to use the newer types of NMR techniques for determining the structure. As will be demonstrated here, when the new techniques are used on a high-field NMR spectrometer, they provide surprisingly simple and unambiguous means for determining the structure of molecules the size of desertomycin.

(1) Uri, J.; Bogнар, R.; Bekesi, I.; Varga, B. *Nature (London)* **1958**, 182, 401.

(2) Bogнар, R.; Sztaricskai, F.; Somogyi, L.; Puskas, M.; Makleit, S. *Acta Chim. Acad. Sci. Hung.* **1968**, 56, 53.

(3) Dolak, L. A.; Reusser, F.; Baczynskyj, L.; Mizsak, S. A.; Hannon, B. R.; Castle, T. M. *J. Antibiot.* **1983**, 36, 13.

(4) Keresztes, T.; Gesztelyi, I.; Bekesi, I.; Korver, A. *Magy. Tud. Akad. Biol. Tud. Oszt. Kozl.* **1982**, 25, 169.

(5) Uri, J.; Herpay, Zs. *Mykosen* **1961**, 4, 128.

(6) Vally-Nagy, T.; Hernady, F.; Szabo, G.; Jeney, A. *Antibiot. Chemother. (Washington, D.C.)* **1961**, 11, 238.

<sup>\*</sup>Laboratory of Chemical Physics, National Institute of Arthritis, Diabetes, and Digestive and Kidney Diseases.

<sup>†</sup>Division of Drug Biology, Food and Drug Administration.

<sup>‡</sup>Antibiotics Research Laboratory.

<sup>±</sup> Present address: Daiichi Seiyaku Co., Tokyo, Japan.